

Finite coupling Kondo insulator transition in the honeycomb lattice

Saeed Saremi and Patrick A. Lee

Department of Physics, Massachusetts Institute of Technology, Cambridge, Massachusetts 02139

(Dated: October 10, 2006)

We study the Kondo-Heisenberg model on the honeycomb lattice at half-filling. Due to the vanishing of the density of states at the fermi level, the Kondo insulator disappears at a finite Kondo coupling even in the absence of the Heisenberg exchange. We adopt a large-N formulation of this model and use the renormalization group machinery to study systematically the second order phase transition of the Kondo insulator (KI) to the algebraic spin liquid (ASL). We find a stable Lorentz-invariant fixed point that controls this second order phase transition. We calculate the exponent ν of the diverging length scale near the transition. The quasi-particle weight of the conduction electron vanishes at this KI-ASL fixed point, indicating non-Fermi liquid behavior. The algebraic decay exponent of the staggered spin correlation is calculated at the fixed point and in the ASL phase. We find a jump in this exponent at the transition point. Plausible scenarios for the phase diagram of the SU(2) model and comparisons to numerical results on the square lattice are discussed.

I. INTRODUCTION

The interplay between charge and spin degrees of freedom has been a focus of research in complex materials such as cuprates and heavy-fermions.¹ The clearest example of this interplay is the quantum critical point seen in many heavy-fermion materials. At zero temperature, the heavy Fermi liquid (HFL) phase disappears exactly at a point where the anti-ferromagnetic (AF) magnetic ordering grows. Non-Fermi liquid behaviors are seen in the quantum critical region, i.e. the V-shaped region above this critical point.¹ The theoretical understanding of why these two seemingly different phases, i.e. AF ordered and heavy fermi liquid, should collapse at one point and a clear understanding of the non-Fermi liquid behaviors in the quantum critical region are poor at the moment.

It is by now understood that the spin density wave approach to understand the quantum critical point in heavy-fermions, known as the Moriya-Hertz-Millis theory², only accounts for small deviations from Fermi liquid theory. New theoretical approaches for understanding the quantum critical heavy-fermions are needed.

In an attempt to find an alternative for the Moriya-Hertz-Millis theory, Senthil *et al.* proposed recently that the AF-HFL transition might be controlled by an *unstable* spin liquid fixed point.^{3,4} This picture is very similar to the Deconfined quantum critical point in the context of the second order phase transition between Neel and valence bond solid (VBS) ground states.¹⁰ In that case the transition to VBS happens due to the existence of an unstable spin liquid on the magnetically disordered side of the critical point. Deconfined quantum critical points open up the possibility of second order phase transitions between “unrelated” phases like AF and HFL. It also has the advantage of giving a plausible scenario for the non-Fermi liquid behavior seen in experiments in heavy fermion materials. This view has had some successes in explaining some of the experimental observations.^{5,6} In this paper, we further explore this point of view.

In search for a microscopic model that provides this type of quantum critical point, we study the Kondo-Heisenberg model on the *honeycomb* lattice at *half-filling*. The heavy fermion quantum critical point in this model is simplified. It corresponds to a point, where both charge gap and spin gap vanishes. This model is given by the following Hamiltonian ($J_K > 0, J_H > 0$):

$$\hat{H} = -t \sum_{\langle ij \rangle, a} \left(c_i^{a\dagger} c_j^a + H.c. \right) + J_K \sum_i \mathbf{s}_i \cdot \mathbf{S}_i + J_H \sum_{\langle ij \rangle} \mathbf{S}_i \cdot \mathbf{S}_j, \quad (1)$$

where i and j live on the honeycomb lattice sites and a is the spin index: $\{\uparrow, \downarrow\}$. The \mathbf{s}_i and \mathbf{S}_i denote the conduction electron spin and the localized spin at the site i respectively. What makes the honeycomb lattice very interesting to study is the fact that the Kondo gap vanishes at a *finite* coupling constant even as $J_H \rightarrow 0$. This is due to the fact that, in contrast to the square lattice, the density of states of the conduction electrons vanishes at the Fermi level.⁷

The Kondo-Heisenberg model on the honeycomb lattice at half-filling is also interesting, because it can be studied by quantum Monte Carlo *without* the fermion sign problem.^{8,9} The present paper can be considered a prelude to such a study. In this connection we mention the quantum Monte Carlo study of the Kondo lattice model ($J_H = 0$) on the square lattice by Assaad.⁹ He found a quantum phase transition of the AF ordered ground state to a disordered one caused by the Kondo exchange. The quasi-particle gap however did not vanish at the transition point,²⁶ i.e. the magnetic transition happened inside the KI phase. This made the transition a magnetic transition belonging to the O(3) non-linear sigma model universality class. Note that the nested Fermi line of the tight-binding band provides the instability towards AF at (π, π) even in the absence of the Heisenberg exchange J_H . In contrast the honeycomb lattice tight binding band has Fermi points in the corner of the Brillouin zone called the Dirac points. This causes the nesting to be extremely weak as compared to the per-

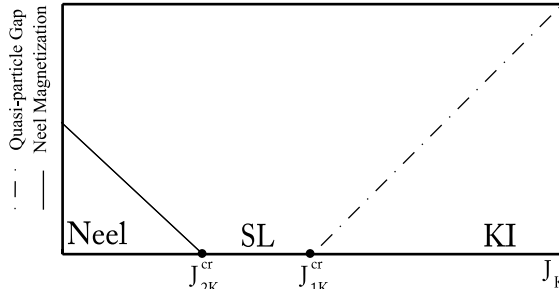


FIG. 1: A scenario for the zero temperature phase diagram of the Kondo-Heisenberg Hamiltonian on the honeycomb lattice at half-filling [given by Hamiltonian Eq. (1)] as a function of J_K ($t = 1$) for a sufficiently small J_H . In contrast to the same model on a square lattice, Kondo gap denoted schematically by the dotted-dashed line vanishes at a finite coupling constant J_{1K}^{cr} . The weak nesting of the Dirac nodes of the honeycomb lattice makes the KI transition to a spin liquid ground state plausible.

fectly nested lines of the Fermi line in the square lattice.

Next we consider different scenarios for the ground state phase diagram of our model, where we consider varying J_K ($t = 1$), keeping J_H to be small. In the first scenario, sketched schematically in Fig. 1, the finite coupling Kondo transition is to a magnetically disordered ground state (spin liquid). In this scenario the AF ordered ground state does not survive up to the KI transition point for sufficiently small J_H . The Kondo physics has stabilized a spin liquid ground state in the region between the KI and AF ground states. The charge gap closes at J_{1K}^{cr} , as the KI gives way to a semi-metal. The spin gap may or may not be finite, depending on the nature of the spin liquid. As J_K is further reduced a transition to the Neel phase occurs. This scenario will of course be very exciting, if a spin liquid can indeed be stabilized as the ground state over some parameter range.

The other exciting possibility is that a continuous transition between two distinct orders (AF and KI) exists over a finite parameter range. This scenario is sketched schematically in Fig. 2. In this scenario SL is unstable to Neel ordering. This will be an example of the deconfined quantum critical point mentioned earlier. Finally, scenarios in which an overlapping region, where a Neel state co-exists with the Kondo insulator (similar to the square lattice result of Assaad⁹); or a first order transition can not be ruled out. With these motivations we now sketch an outline of this paper.

In this paper we begin by a mean-field study of the Kondo-Heisenberg model Eq. (1) on the honeycomb lattice. We adopt a fermionic representation for localized spins. We make a mean-field decoupling of $\mathbf{S}_i \cdot \mathbf{S}_j$ in the fermionic hopping channel. This is sometimes referred to as the resonating valence bond (RVB) decoupling. The Kondo interaction is decoupled in the usual mean-field way with the hybridization “order parameter” $b = \left\langle \sum_a f_i^{a\dagger} c_i^a \right\rangle$. The nonzero b will correspond to the KI phase, where the gap in the dispersion is proportional

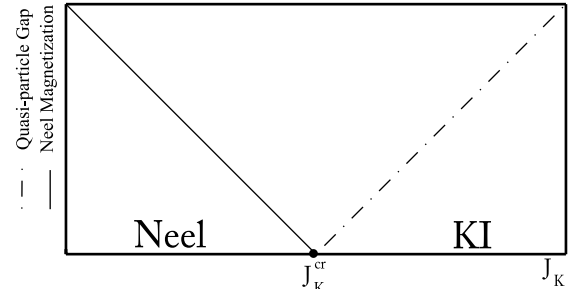


FIG. 2: Another scenario for the zero-temperature phase diagram for the Kondo-Heisenberg Hamiltonian at half-filling on the honeycomb lattice for some (maybe “fine tuned”) Heisenberg exchange J_H as a function of J_K . In contrast to the same model on a square lattice, both the quasi-particle gap denoted schematically by the dotted-dashed line and Neel order parameter denoted by the solid line vanishes at $J_K = J_K^{cr}$.

to b . For any $J_H > 0$ we find a continuous transition between the KI ($b \neq 0$) and a spin liquid state. This spin liquid is characterized by Dirac fermions coupled to U(1) gauge field, and has been called the algebraic spin liquid (ASL), because the spin correlation decays as a power law and spin excitations are gapless.¹² Thus our mean-field theory supports the scenario shown in Fig. 1.

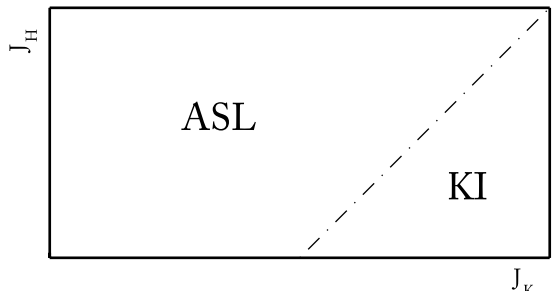


FIG. 3: The mean-field phase diagram of the Hamiltonian given by Eq. (1) in the J_K — J_H space ($t = 1$). For any $J_H > 0$, we find a transition from the KI to the algebraic spin liquid.

The rest of the paper is devoted to studying the critical properties of the fixed point that controls the transition from the KI to ASL. In Sec. II B we generalize our model by letting the spin indices to run from 1 to N rather than just “up” and “down”. The saddle point approximation (i.e. the mean-field) becomes exact as $N \rightarrow \infty$. In Sec. III we derive the low-energy Lagrangian density which sets the stage for a systematic $1/N$ expansion.

Section IV develops the propagator for the Kondo field b , and the gauge field a_μ in the leading order. The Kondo field propagator can be tuned to a massless point at $J_K = J_K^{cr}$. In the $J > J_K^{cr}$ regime the b field condenses to $|b|$ and we will be in the Higgs phase where the gauge field is massive. This is nothing but the Kondo physics, where the excitation gap is proportional to $|b|$. In the $J < J_K^{cr}$ regime the Kondo field is not consensed, and is massive. The physics is described by Dirac fermions coupled to a U(1) gauge field. This field theory, known as QED₃, has been studied extensively^{12–16}, and is understood to

be an algebraic spin liquid due to algebraic correlation of spins.¹² This phase is believed to be deconfined.¹³

Section V A contains the main technical calculation of this paper. We calculate the exponent ν , which describes the diverging length scale of the transition. We consider a relativistic fixed point, which allows us to adopt standard field theory methods. In Sec. V B we calculate the decay exponent of the staggered localized spin. In Sec. VI we show that the relativistic fixed point is stable and is therefore the appropriate fixed point to study for the transition.

II. FINITE COUPLING KONDO TRANSITION

A. Mean-Field Transition

Our starting point is the Hamiltonian

$$\hat{H} = -t \sum_{\langle ij \rangle, a} \left(c_i^{a\dagger} c_j^a + H.c. \right) + J_K \sum_i \mathbf{s}_i \cdot \mathbf{S}_i + J_H \sum_{\langle ij \rangle} \mathbf{S}_i \cdot \mathbf{S}_j, \quad (2)$$

where i and j live on the honeycomb lattice sites and a is the spin index: $\{\uparrow, \downarrow\}$. The \mathbf{s}_i denotes the conduction electron spin at the site i and the capital \mathbf{S}_i denotes the localized spin at the site i and they both are SU(2) spins with an SU(2) spin algebra. The conduction electron spin is given by

$$\mathbf{s}_i = \frac{1}{2} c_i^{a\dagger} \boldsymbol{\sigma}_{ab} c_i^b, \quad (3)$$

where $\boldsymbol{\sigma} = (\sigma_x, \sigma_y, \sigma_z)$ are the Pauli matrices. We adopt a fermionic representation for localized spins, where their Hilbert space $\{|\uparrow\downarrow_i\rangle, |\downarrow\uparrow_i\rangle\}$, is constructed using Fermionic operators:

$$\begin{aligned} |\downarrow\downarrow_i\rangle &= f_i^{\downarrow\dagger} |0\rangle, \\ |\uparrow\uparrow_i\rangle &= f_i^{\uparrow\dagger} |0\rangle. \end{aligned} \quad (4)$$

The anti-commutation relation:

$$\{f_i^{a\dagger}, f_j^b\} = \delta_{ab} \delta_{ij} \quad (5)$$

together with

$$\mathbf{S}_i = \frac{1}{2} f_i^{a\dagger} \boldsymbol{\sigma}_{ab} f_i^b \quad (6)$$

will result in the SU(2) commutation relations for spin \mathbf{S} . However, the Hilbert space of the *localized* spin \mathbf{S}_i is restricted to only two elements: $\{|\uparrow\downarrow_i\rangle, |\downarrow\uparrow_i\rangle\}$. Therefore identifying localized spin by fermionic operators given by Eq. (6) has to be accompanied by the constraint

$$\sum_a f_i^{a\dagger} f_i^a = 1. \quad (7)$$

Combining Eqs. (3) — (7); together with the following identity for the Pauli matrices

$$\boldsymbol{\sigma}_{ab} \cdot \boldsymbol{\sigma}_{cd} = 2\delta_{ad}\delta_{bc} - \delta_{ab}\delta_{cd} \quad (8)$$

one finds a fermionic representation of the spin–spin interactions in the Hamiltonian of Eq. (2):

$$\mathbf{s}_i \cdot \mathbf{S}_i = -\frac{1}{4} \left[\left(c_i^{a\dagger} f_i^a \right) \left(f_i^{b\dagger} c_i^b \right) + H.c. \right] + \frac{1}{4}, \quad (9)$$

$$\mathbf{S}_i \cdot \mathbf{S}_j = -\frac{1}{4} \left[\left(f_i^{a\dagger} f_j^a \right) \left(f_j^{b\dagger} f_i^b \right) + H.c. \right] + \frac{1}{4}, \quad (10)$$

where the sum over the spin indices is understood.

The four-fermion interaction terms of Eqs. 9 and 10 will be replaced in the mean-field (MF) simplification by a quadratic interaction:

$$\hat{A} = \hat{A}_1 \hat{A}_2 \rightarrow \langle A_1 \rangle \hat{A}_2 + \hat{A}_1 \langle A_2 \rangle - \langle A_1 \rangle \langle A_2 \rangle, \quad (11)$$

where \hat{A} denotes a generic four-fermion interaction term. To make the interaction quadratic one has to ignore $(A_1 - \langle A_1 \rangle)(A_2 - \langle A_2 \rangle)$. So the mean-field parameters have to satisfy the self-consistency condition:

$$\frac{\partial F_{MF}}{\partial \langle A_i \rangle} = \langle \hat{A}_i - \langle A_i \rangle \rangle = 0. \quad (12)$$

We make the interaction terms given by Eqs. (9) and (10) quadratic by choosing the following mean-field parameters:

$$\left\langle \sum_a c_i^{a\dagger} f_i^a \right\rangle = -|b_i| e^{i\theta_i}, \quad (13)$$

$$\left\langle \sum_a f_i^{a\dagger} f_j^a \right\rangle = -|\chi_{ij}| e^{ia_{ij}}. \quad (14)$$

The first parameter $|b_i| e^{i\theta_i}$ lives on sites. The second parameter $|\chi_{ij}| e^{ia_{ij}}$ lives on links. We assume that these parameters have a constant magnitude throughout the lattice. When they take a non-zero value, small deviations from their “constant” magnitudes cost energy: they are locally stable. $|b_i| = b \neq 0$ corresponds to the Kondo insulator phase, where the gap in the excitations is proportional to b . We also note that the conventional decoupling of $\mathbf{S}_i \cdot \mathbf{S}_j$ leads to the anti-ferromagnetic order parameter $\langle S_{iz} \rangle$. In this paper we adopt the alternative decoupling of Eq. (14), which is often called the RVB (Resonating Valence Bond) decoupling. RVB decoupling leads to a spin liquid state.

The U(1) gauge freedom in defining f gives the freedom to eliminate θ_i by the following gauge transformation:

$$\begin{aligned} f_i^a &\rightarrow e^{i\theta_i} f_i^a, \\ a_{ij} &\rightarrow a_{ij} + (\theta_i - \theta_j). \end{aligned} \quad (15)$$

This transformation leaves the total flux modulo 2π

$$\sum_{\bigcirc} a_{ij} \pmod{2\pi} \quad (16)$$

through any closed loop invariant. Next we make a choice $\chi_{ij} = \chi$ where χ is real. This choice corresponds to the

case where the total flux through each hexagon modulo 2π is zero.

Our mean-field choices result in the following mean-field Hamiltonian:

$$\begin{aligned}\hat{H}_{MF} = & -t \sum \left(c_i^{a\dagger} c_j^a + H.c. \right) \\ & + \frac{J_K b}{2} \sum \left(f_i^{a\dagger} c_i^a + H.c. \right) \\ & + \frac{J_H \chi}{2} \sum \left(f_i^{a\dagger} f_j^a + H.c. \right) \\ & + \mathcal{N} \left(J_K b^2 + \frac{3J_H}{2} \chi^2 \right),\end{aligned}\quad (17)$$

where \mathcal{N} is the number of unit cells. The different coefficients of the constant terms are due to the fact that there are 2 sites as opposed to 3 links per unit cell. We also mention that, at the mean-field level, the constraint given by Eq. (7) is enforced on average by having a chemical potential for f fermions. This chemical potential is zero due to f-fermions particle-hole symmetry.

From \hat{H}_{MF} , the MF free energy can be calculated numerically. MF parameters satisfying the self consistency condition are then obtained. The numerics confirm the finite coupling Kondo transition in a background χ , for any $J_H > 0$. Next we show this finite coupling Kondo transition analytically and find the exponent β

$$|b| \propto (J_K - J_K^{cr})^\beta, \quad (18)$$

by focusing on the low-energy theory near the Dirac nodes.

We focus first on the c electrons kinetic term $-t \sum (c_i^{a\dagger} c_j^a + H.c.)$. We do the Fourier transformation

$$c_A(\mathbf{k}) = \frac{1}{\mathcal{N}} \sum_{\mathbf{R}} e^{i\mathbf{k}\cdot\mathbf{R}} c_A(\mathbf{R}) \quad (19)$$

where \mathbf{R} are the Bravais lattice vectors and $c_A(\mathbf{R})$ is the conduction electron annihilation operator at the A sublattice site of the unit cell positioned at \mathbf{R} . The similar transformation is done to get $c_B(\mathbf{k})$. Conduction electrons kinetic term in momentum space will take the form:

$$- \sum_{\langle ij \rangle} t c_i^\dagger c_j + H.c. = -t \sum_{\mathbf{k}} \Gamma(\mathbf{k}) c_A^\dagger(\mathbf{k}) c_B(\mathbf{k}) + H.c., \quad (20)$$

where

$$\Gamma(\mathbf{k}) = 1 + e^{i\mathbf{k}\cdot(\eta_2 - \eta_1)} + e^{-i\mathbf{k}\cdot(2\eta_1 + \eta_2)}, \quad (21)$$

and $\eta_1 = l(1, 0)$ and $\eta_2 = l(-1/2, \sqrt{3}/2)$ are two of the three vectors that connect A sublattice sites to nearest neighbor B sublattice sites. l is the length between nearest neighbor sites which will be set to the unit length: $l = 1$.

$\Gamma(\mathbf{k})$ vanishes at the Dirac nodes $\pm\mathbf{k}_D$, which is given by

$$\mathbf{k}_D = (0, \frac{4\pi}{3\sqrt{3}}). \quad (22)$$

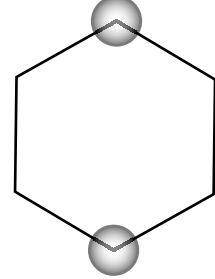


FIG. 4: The Brillouin zone of the honeycomb lattice. Corners of the Brillouin zone is where the tight-binding gap vanishes. The *independent* low-energy modes are denoted by the filled-circles around the two Dirac nodes $\pm\mathbf{k}_D$.

Near the nodes as schematically represented by the filled circles in the Fig. 4, $\Gamma(\pm\mathbf{k}_D + \mathbf{q})$ is given by

$$\Gamma(\pm\mathbf{k}_D + \mathbf{q}) = \frac{3}{2}(iq_1 \mp q_2) + \mathcal{O}(\mathbf{q}^2). \quad (23)$$

To write the conduction electron kinetic term near the Dirac nodes, we use the following notation, which will also be helpful in Sec. III:

$$\psi_{\pm}(\mathbf{q}) \equiv \begin{bmatrix} c_A(\pm\mathbf{k}_D + \mathbf{q}) \\ c_B(\pm\mathbf{k}_D + \mathbf{q}) \end{bmatrix} \quad (24)$$

After collecting Eqs. (20) — (24), we get

$$\begin{aligned}- \sum_{\langle ij \rangle} t c_i^\dagger c_j + H.c. \sim & \frac{3t}{2} \sum_{\mathbf{q}} \psi_+(\mathbf{q})^\dagger (q_1 \sigma_2 + q_2 \sigma_1) \psi_+(\mathbf{q}) \\ & + \frac{3t}{2} \sum_{\mathbf{q}} \psi_-(\mathbf{q})^\dagger (q_1 \sigma_2 - q_2 \sigma_1) \psi_-(\mathbf{q}),\end{aligned}\quad (25)$$

where “~” is used, since in contrast to Eq. (20) the momentum sum is restricted to be near the Dirac nodes.

Next we obtain the energy dispersion near the node $+\mathbf{k}_D$. The MF Hamiltonian in momentum space and near the node $+\mathbf{k}_D$, denoted by $\hat{H}_+(\mathbf{q})$, is given by

$$\hat{H}_+(\mathbf{q}) = [\psi_+(\mathbf{q})^\dagger \ \phi_+(\mathbf{q})^\dagger] \mathcal{H}_+ \begin{bmatrix} \psi_+(\mathbf{q}) \\ \phi_+(\mathbf{q}) \end{bmatrix}, \quad (26)$$

where we have droped the constant term of Eq. (17) and we have used a similar notation as in Eq (24) for the f fermions:

$$\phi_{\pm}(\mathbf{q}) \equiv \begin{bmatrix} f_A(\pm\mathbf{k}_D + \mathbf{q}) \\ f_B(\pm\mathbf{k}_D + \mathbf{q}) \end{bmatrix}. \quad (27)$$

The 4×4 matrix \mathcal{H}_+ is given in block form by

$$\mathcal{H}_+ = \frac{1}{2} \begin{bmatrix} 2v_c(q_1 \sigma_2 + q_2 \sigma_1) & J_K b \\ J_K b & -2v_f(q_1 \sigma_2 + q_2 \sigma_1) \end{bmatrix}, \quad (28)$$

where v_c and v_f are given by:

$$v_c = \frac{3}{2}t, \quad (29)$$

$$v_f = \frac{3}{4}\chi J_H. \quad (30)$$

It will be clear why notations v_c and v_f is used shortly. It is straightforward to diagonalize the above matrix. The four eigenvalues are given by:

$$e(\mathbf{q}) = \pm \left((v_c - v_f)|\mathbf{q}| \pm \sqrt{(v_f + v_c)^2 \mathbf{q}^2 + J_K^2 b^2} \right) / 2. \quad (31)$$

We have dropped the subscript + from $e(\mathbf{q})$, since the dispersion near the other node is the same.

To understand the above dispersion better, we mention its behavior in different regimes:

- $b = 0$. The MF Hamiltonian has two decoupled parts: kinetic terms for the conduction electrons and for f fermions. In this case the 4 eigenvalues near the nodes become $\pm v_c |\mathbf{q}|$ and $\pm v_f |\mathbf{q}|$. They are the massless dirac dispersions for conduction electrons c and fermions f with *velocities* v_c and v_f respectively. The phase with $b = 0$ is an algebraic spin liquid phase as will be clear in Sec. V B. This is closely related to the work of Rantner and Wen where Dirac fermions coupled to a gauge field was found to be an algebraic spin liquid.¹²
- $v_f = v_c, b \neq 0$. The dispersion is the *massive relativistic* Dirac dispersion

$$e(\mathbf{q}) = \pm \sqrt{v_c^2 \mathbf{q}^2 + (J_K b/2)^2}, \quad (32)$$

where each eigenvalue is doubly degenerate. $J_K b/2$ is the mass of our relativistic quasi-particles. In Sec. III, we will see that the low-energy theory, in the limit $v_f = v_c$, is Lorentz invariant. The above relativistic dispersion is a sign of this Lorentz invariance.

- *sign of v_f* . The sign of χ (v_f) has dramatic consequences on the shape of the dispersion and also on the continuum formulation of the model near the phase transition. Due to the coupling between f-fermions and the conduction electrons the free energy is not invariant under the mapping $\chi \mapsto -\chi$. In the Kondo insulating phase ($b \neq 0$); the dispersion for $v_f > 0$ is gapped. However the dispersion for $v_f < 0$ has a gapless ring around each Dirac node with the radius

$$q_c = \frac{J_K b}{2\sqrt{-v_c v_f}}. \quad (33)$$

It turns out that the positive (self consistent) χ ($v_f > 0$) is *more stable*. This is not surprising from the above fact that the dispersion for $v_f > 0$ is gapped as opposed to $v_f < 0$ which is gapless. We are only concerned with the stable solution $\chi > 0$ in this paper.

The MF transition at zero temperature can be analyzed by minimizing the total energy

$$E = 4 \sum_{e(\mathbf{q}) < 0} e(\mathbf{q}) + \mathcal{N} \left(J_K b^2 + \frac{3J_H}{2} \chi^2 \right), \quad (34)$$

$$\frac{\partial E}{\partial b} = 0, \text{ and } \frac{\partial E}{\partial \chi} = 0. \quad (35)$$

The coefficient $4 = 2 \times 2$ is for counting spins and the two nodes. The condition $\frac{\partial E}{\partial \chi} = 0$ at $b = 0$ results in the self consistent χ , which varies slowly across the transition. For $v_f > 0$, the negative energy bands are given by $(\pm(v_c - v_f)|\mathbf{q}| - \sqrt{(v_f + v_c)^2 \mathbf{q}^2 + J_K^2 b^2}) / 2$. Therefore

$$\sum_{e(\mathbf{q}) < 0} e(\mathbf{q}) = - \sum_{\mathbf{q}} \sqrt{(v_f + v_c)^2 \mathbf{q}^2 + J_K^2 b^2}. \quad (36)$$

Combine Eqs. 34 — 36, to arrive at the self-consistency equation for b :

$$\frac{2}{\mathcal{N}} \sum_{\mathbf{q}} \frac{J_K}{\sqrt{(v_f + v_c)^2 \mathbf{q}^2 + J_K^2 b^2}} = 1. \quad (37)$$

It is clear from the above equation that the Kondo phase does not survive down to $J_K = 0$, in contrast to the case when the conduction band possess a *Fermi surface*. The Kondo insulator phase disappears at a *finite* coupling constant J_K^{cr} . Taking the limit $\mathcal{N} \rightarrow \infty$, we find the following dependance of the Kondo parameter $|b|$ as a function of the distance from the transition $J_K - J_K^{cr}$:

$$|b| \propto (J_K - J_K^{cr}), \quad (38)$$

$$J_K^{cr} = \frac{v_c + v_f}{\Lambda},$$

where $\Lambda \ll 1$ is a large-momentum cutoff around the Dirac nodes $\pm \mathbf{k}_D$.

To summarize, the MF solution has two interesting features:

- The Kondo insulator phase disappears at a finite coupling constant.
- The Kondo condensate $|b|$ vanishes linearly as the distance from the critical point. We emphasize that a Landau-type expansion for the b mean-field parameter would yield the result $|b| \propto (J_K - J_K^{cr})^{1/2}$ near the transition point. The appearance of non-trivial critical exponent at the mean-field level is characteristic of the coupling of b to gapless fermions which is addressed systematically in the $1/N$ expansion.

B. Large N Formulation : Mean-Field Justified

In this section we extend the physical model with two spin-flavors to a generalized model with N spin-flavors.¹¹

We show that the mean-field solution is the stable solution in the infinite N limit.

The conduction electrons kinetic term $\sum (c_i^{a\dagger} c_j^a + H.c.)$ is already in the generalized form. We just let the spin index a to run from 1 to N . The spin–spin interactions as written in Eqs. 9 and 10 is also easily generalized by letting the spin indices to run from 1 to N . In addition we *control* these interactions by replacing $\frac{1}{2}$ with $\frac{1}{N}$. So the generalized version of the Hamiltonian of Eq. (2) is given by

$$\begin{aligned} \hat{H} = & -t \sum_{\langle ij \rangle} (c_i^{a\dagger} c_j^a + H.c.) \\ & - \frac{J_K}{2N} \sum_i [(c_i^{a\dagger} f_i^a)(f_i^{b\dagger} c_i^b) + H.c.] \\ & - \frac{J_H}{2N} \sum_{\langle ij \rangle} [(f_i^{a\dagger} f_j^a)(f_j^{b\dagger} f_i^b) + H.c.], \end{aligned} \quad (39)$$

where the sum over spin indices is understood. The above Hamiltonian has to accompanied by the local constraint:

$$\sum_a f_i^{a\dagger} f_i^a = \frac{N}{2}. \quad (40)$$

The above generalized model will coincide with the Hamiltonian Eq. (2) for $N=2$. In fermion coherent state representation, using Grassmann variables, the Euclidean Lagrangian and the partition function take the form

$$\begin{aligned} L_E([c, f, a_0]) = & \sum_i \left(\bar{c}_i^a(x_0) \partial_0 c_i^a(x_0) + \bar{f}_i^a(x_0) \partial_0 f_i^a(x_0) \right. \\ & \left. - ia_{i0} \left(\bar{f}_i^a(x_0) f_i^a(x_0) - \frac{N}{2} \right) \right) + H, \\ Z = & \int \mathcal{D}[\bar{c} \bar{f} f a_0] e^{- \int dx_0 L_E(x_0)}, \end{aligned} \quad (41)$$

where x_0 denotes the imaginary time. The field a_{i0} , when integrated over, will produce delta functions at each site enforcing the local constraint given by Eq. 40. The notation a_{i0} is used because it will serve as the *time* component of the emergent gauge field.

Next we do the standard Hubbard–Stratonovich transformation to decouple the four-fermion terms in the action at a cost of introducing the complex fields b_i , which

lives on sites and χ_{ij} , which lives on links:

$$\begin{aligned} L_E([c, f, b, \chi, a_0]) = & \sum_i \bar{c}_i^a \partial_0 c_i^a - t \sum_{\langle ij \rangle} (\bar{c}_i^a c_j^a + c.c.) \\ & + \sum_i \left(\bar{f}_i^a (\partial_0 - ia_{i0}) f_i^a + iNa_{i0}/2 \right) \\ & + \sum_{\langle ij \rangle} \left(\frac{N}{J_H} |\chi_{ij}|^2 + \chi_{ij} \bar{f}_i^a f_j^a + \chi_{ij}^* \bar{f}_j^a f_i^a \right) \\ & + \sum_i \left(\frac{N}{J_K} |b_i|^2 + b_i \bar{c}_i^a f_i^a + b_i^* \bar{f}_i^a c_i^a \right), \end{aligned} \quad (42)$$

$$Z = \int \mathcal{D}[\bar{c} \bar{f} f b \chi^* \chi a_0] e^{- \int dx_0 L_E(x_0)}.$$

The x_0 dependance of Grassmann and complex fields in the Lagrangian is understood as well as the droped indices in the measure of the path integral.

The action is quadratic in the Fermionic fields and it can be integrated out at the cost of obtaining an effective action for b_i and χ_{ij} fields, which is highly *nonlocal*. Since there is no mixing of different spin-flavors, the resulting effective action will be proportional to N :

$$\frac{L_E([b, \chi])}{N} = \log \det \mathcal{M} + \frac{1}{J_K} \sum_i |b_i|^2 + \frac{1}{J_H} \sum_{\langle ij \rangle} |\chi_{ij}|^2. \quad (43)$$

\mathcal{M} is a $4N \times 4N$ Hermitian matrix, which encodes the quadratic interaction of the fermionic fields as given by Eq. (42), e.g. $\mathcal{M}_{\bar{c}_i f_i} = b_i$.²² The “ $\det \mathcal{M}$ ” makes the effective Lagrangian in terms of b_i and χ_{ij} fields nonlocal.

The saddle point approximation for the above Lagrangian $L_E([b, \chi])$ is exact as $N \rightarrow \infty$. The saddle point equations will be the mean-field equations given by Eq. (12), and this is how the mean-field developed in the previous section is justified. Furthermore the Lagrangian given in Eq. (42) will set the stage for a systematic $1/N$ expansion around the mean-field solution.

III. BEYOND MEAN-FIELD: LOW-ENERGY EFFECTIVE FIELD THEORY

In this section we obtain the Lagrangian density near the critical point starting from the microscopic Lagrangian. There are two independent nodes $\pm \mathbf{k}_D$ and near each node there are fermions from A and B sublattices. We package these c and f fermions into four component spinors Ψ and Φ . This is done in a way to make the kinetic terms for both fields look the same.

Since there is no mixing of different spin-flavors in the microscopic Lagrangian Eq. (42), we will drop this index through the derivation of the Lagrangian density. The spin-flavor index will be resurrected at the end.

The kinetic term for the conduction electrons was discussed in Sec. II A:

$$\begin{aligned} -t \sum c_i^\dagger c_j + H.c. &\sim v_c \sum_{\mathbf{q}} \psi_+(\mathbf{q})^\dagger (q_1 \sigma_2 + q_2 \sigma_1) \psi_+(\mathbf{q}) \\ &+ v_c \sum_{\mathbf{q}} \psi_-(\mathbf{q})^\dagger (q_1 \sigma_2 - q_2 \sigma_1) \psi_-(\mathbf{q}) \end{aligned} \quad (44)$$

Note that under the transformation $\psi_-(\mathbf{q}) \rightarrow \sigma_2 \psi_-(\mathbf{q})$ the second term has the same form as the first one. We combine the two 2-component spinors, associated with the two Dirac nodes, to form a 4-component spinor $\Psi(\mathbf{q})$:

$$\Psi(\mathbf{q}) \equiv \begin{bmatrix} \psi_+(\mathbf{q}) \\ \sigma_2 \psi_-(\mathbf{q}) \end{bmatrix}. \quad (45)$$

To write the kinetic term in terms of $\Psi(\mathbf{q})$, we define the 4×4 block diagonal matrices τ_i :

$$\tau_i \equiv \begin{bmatrix} \sigma_i & 0 \\ 0 & \sigma_i \end{bmatrix} = \sigma_i \otimes \mathbf{1}_{2 \times 2}. \quad (46)$$

The kinetic term then takes the form

$$-t \sum c_i^\dagger c_j + H.c. \sim v_c \sum_{\mathbf{q}} \Psi(\mathbf{q})^\dagger (q_1 \tau_2 + q_2 \tau_1) \Psi(\mathbf{q}). \quad (47)$$

After taking the continuum limit, the Lagrangian density corresponding to this Hamiltonian is:

$$\mathcal{L}_E^{(1)} = \Psi^\dagger \partial_0 \Psi - i v_c \Psi^\dagger (\tau_2 \partial_1 + \tau_1 \partial_2) \Psi. \quad (48)$$

To use the field theory techniques one would write $\mathcal{L}_E^{(1)}$ in a different form

$$\mathcal{L}_E^{(1)} = \bar{\Psi} \tau_3 \partial_0 \Psi + v_c \bar{\Psi} (-\tau_1 \partial_1 + \tau_2 \partial_2) \Psi, \quad (49)$$

where $\bar{\Psi}$ is defined to be

$$\bar{\Psi} \equiv \Psi^\dagger \tau_3. \quad (50)$$

Next we focus on $\sum (\chi_{ij} \bar{f}_i^a f_j^a + \chi_{ij}^* \bar{f}_j^a f_i^a)$ term in Eq. (42). Consider the mean-field case $\chi_{ij} = \chi > 0$. The phase fluctuations will be included as gauge field fluctuations later on. Ignoring the phase fluctuations, this term looks exactly like the kinetic term of the conduction electrons given by Eq. (44), but with an opposite sign:

$$\begin{aligned} \chi \sum f_i^\dagger f_j + H.c. &\sim v_f \sum_{\mathbf{q}} \phi_+(\mathbf{q})^\dagger (-q_1 \sigma_2 - q_2 \sigma_1) \phi_+(\mathbf{q}) \\ &+ v_f \sum_{\mathbf{q}} \phi_-(\mathbf{q})^\dagger (-q_1 \sigma_2 + q_2 \sigma_1) \phi_-(\mathbf{q}). \end{aligned} \quad (51)$$

We make this look like Eq. (47) by a further transformation to absorb the minus sign and we again combine the 2-component spinors near the two nodes to form a 4-component spinor $\Phi(\mathbf{q})$:

$$\Phi(\mathbf{q}) \equiv \begin{bmatrix} \sigma_3 \phi_+(\mathbf{q}) \\ -i \sigma_1 \phi_-(\mathbf{q}) \end{bmatrix}. \quad (52)$$

On the grounds of gauge invariance, we write the Lagrangian density corresponding to the “kinetic” term of the f fermions

$$\mathcal{L}_E^{(2)} = \bar{\Phi} \tau_3 (\partial_0 - i a_0) \Phi + v_f \bar{\Phi} \left(-\tau_1 (\partial_1 - i a_1) + \tau_2 (\partial_2 - i a_2) \right) \Phi, \quad (53)$$

where the non-compact gauge field $\mathbf{a}(\mathbf{x})$ appears as a connection to produce covariant derivative. It is related to the the phase a_{ij} through the relation $\mathbf{a}(\mathbf{x}) = a_{ij} \hat{\eta}_{ij}$, where $\hat{\eta}_{ij}$ is the unit vector connecting the site i to the site j . We have used the same definition as in Eq. (50):

$$\bar{\Phi} \equiv \Phi^\dagger \tau_3. \quad (54)$$

En route to the continuum limit, we have implicitly dropped the compact character of the gauge field. This is only valid if the gauge fluctuations are not very strong. In the imaginary time evolution, there will be events on the lattice scale that change the flux of the gauge field by 2π . If these events do not proliferate, we will be in small gauge coupling constant regime and taking the continuum limit is justified.¹⁹ We return to this point at the end of this section.

Now we focus on the interaction term $\sum_i b_i c_i^\dagger f_i$. We write this in the momentum space and restrict c and f fermions momentum to be near $\pm \mathbf{k}_D$, and b momentum to be near $k = 0$. Simple manipulations

$$\psi_+^\dagger(\mathbf{q}) \phi_+(\mathbf{q}') = \psi_+^\dagger(\mathbf{q}) \sigma_3 (\sigma_3 \phi_+(\mathbf{q}')), \quad (55)$$

$$\psi_-^\dagger(\mathbf{q}) \phi_-(\mathbf{q}') = (\sigma_2 \psi_-(\mathbf{q}))^\dagger \sigma_3 (-i \sigma_1 \phi_-(\mathbf{q}')), \quad (56)$$

combined with the definitions for Ψ and Φ fields, result in

$$\begin{aligned} \psi_+^\dagger(\mathbf{q}) \phi_+(\mathbf{q}') + \psi_-^\dagger(\mathbf{q}) \phi_-(\mathbf{q}') &= \Psi^\dagger(\mathbf{q}) \tau_3 \Phi(\mathbf{q}') \\ &= \bar{\Psi}(\mathbf{q}) \Phi(\mathbf{q}'). \end{aligned} \quad (57)$$

Therefore in the continuum limit the Lagrangian density corresponding to $\sum_i (b_i c_i^\dagger f_i + b_i^* f_i^\dagger c_i)$ will be

$$\mathcal{L}_E^{(3)} = b \bar{\Psi} \Phi + b^* \bar{\Phi} \Psi. \quad (58)$$

Now collect $\mathcal{L}_E^{(1)}$, $\mathcal{L}_E^{(2)}$ and $\mathcal{L}_E^{(3)}$, to write the Lagrangian density

$$\begin{aligned} \mathcal{L}_E^{v_c/v_f} &= \bar{\Psi}^a \gamma_\mu^{v_c/v_f} \partial_\mu \Psi^a + \bar{\Phi}^a \gamma_\mu (\partial_\mu - i a_\mu) \Phi^a \\ &+ b \bar{\Psi}^a \Phi^a + b^* \bar{\Phi}^a \Psi^a + \frac{N}{J_K} |b|^2 + \dots, \end{aligned} \quad (59)$$

where the spin indices are restored. γ_μ^ϱ is defined to be

$$\gamma_\mu^\varrho \equiv (\tau_3, -\varrho \tau_1, \varrho \tau_2), \quad (60)$$

and γ_μ is a shorthand for γ_μ^ϱ with $\varrho = 1$. The velocity v_f in Eq. (53) is absorbed by scaling \mathbf{x} and \mathbf{a} . As a result, the velocities enter only as the dimensionless ratio v_c/v_f via $\gamma_\mu^{v_c/v_f}$.

Taking the continuum limit, which is essentially a coarse graining process, generates new interactions among coarse grained fields.²⁰ The ellipsis in Eq. (59) denotes such new interactions. Not all possible terms are allowed though. Since the coarse graining process does not break symmetries of the microscopic Lagrangian, the generated interactions should respect these symmetries.¹⁷

Next we set $v_f = v_c$ to make the low-energy theory Lorentz symmetric. The action in the presence of *two different velocities* will not respect the Lorentz symmetry. Under RG transformation — in the absence of Lorentz symmetry — the velocities *will* change, since there is no symmetry to protect them from changing. We shall show later that the Lorentz invariance is protected in the RG sense, in that small deviation from $v_f = v_c$ will scale to zero under RG transformation. Thus we focus our discussion on this Lorentz invariant fixed point.

The Lorentz-symmetric Lagrangian density is given by:

$$\begin{aligned} \mathcal{L}_E = & \bar{\Psi}^a \gamma_\mu \partial_\mu \Psi^a + \bar{\Phi}^a \gamma_\mu (\partial_\mu - ia_\mu) \Phi^a \\ & + b \bar{\Psi}^a \Phi^a + b^* \bar{\Phi}^a \Psi^a + \frac{N}{J_K} |b|^2 \\ & + \frac{N}{2e^2} (\epsilon_{\mu\nu\lambda} \partial_\nu a_\lambda)^2 + Ng|(\partial_\mu + ia_\mu) b|^2 + \dots, \end{aligned} \quad (61)$$

where \mathcal{L}_E is a shorthand for \mathcal{L}_E^q with $q = 1$. The last two terms are two examples of the terms that will be generated in the coarse graining process. They are written on the grounds of gauge invariance. In Sec. VI we show that these new terms and other terms grouped in the ellipsis are irrelevant at our finite coupling Kondo transition fixed point. Embedded in Eq. (61), is the QED₃ Lagrangian density

$$\bar{\Phi}^a \gamma_\mu (\partial_\mu - ia_\mu) \Phi^a + \frac{N}{2e^2} (\epsilon_{\mu\nu\lambda} \partial_\nu a_\lambda)^2 + \dots. \quad (62)$$

QED₃ has been studied before as the low-energy theory of the staggered flux phase^{12–14}. We have used the recent result¹³ about the irrelevance of instanton events near the QED₃ fixed point and took the gauge field to be non-compact. In our formulation the *physical* SU(2) theory corresponds to N=2 *four*-component spinors. It could have been formulated as $N_f = 4$ *two*-component spinors near each node in the Brillouin zone. To go back and forth between these formulations one just needs to use $N_f = 2N$.

IV. 1/N SYSTEMATIC EXPANSION: FIELD PROPAGATORS

The Lagrangian density Eq. (61), derived in the previous section, allows us to develop the machinery of 1/N expansion. The propagators for the fields b and a_μ are of order 1/N in the large N limit. This will allow us to calculate different propagators and scaling dimensions order by order in 1/N.

We start with our notations for propagators of the fermion fields, Ψ and Φ . We use a single line notation for

the Φ field propagator and a double-line for Ψ propagator:

$$\langle \Psi_i^a \bar{\Psi}_j^b \rangle (q) = i \overline{\text{---}}^q \text{---} j = \delta^{ab} (iq)_{ij}^{-1}, \quad (63)$$

$$\langle \Phi_i^a \bar{\Phi}_j^b \rangle (q) = i \overline{\text{---}}^q \text{---} j = \delta^{ab} (iq)_{ij}^{-1}, \quad (64)$$

where Feynman's slash notation

$$q = q_\mu \gamma_\mu \quad (65)$$

is used.

The Gauge Field a_μ . Our Lagrangian density \mathcal{L}_E has a QED₃ piece

$$\bar{\Phi}^a \gamma_\mu (\partial_\mu - ia_\mu) \Phi^a + \frac{N}{2e^2} (\epsilon_{\mu\nu\lambda} \partial_\nu a_\lambda)^2 + \dots, \quad (66)$$

which has been studied before.^{12–16} We refer the reader to the Appendix B of Ref. 14 for the calculation of the QED₃ gauge propagator. The QED₃ gauge propagator, in the leading order, is given by:

$$\langle a_\mu a_\nu \rangle (q) = \mu \overbrace{\text{---}}^q \text{---} \nu = \frac{8}{N|q|} \left(\delta_{\mu\nu} + \frac{q_\mu q_\nu}{q^2} (\xi - 1) \right), \quad (67)$$

where ξ is the Fadeev-Popov gauge fixing parameter. $\xi = 1$ corresponds to the Feynman gauge and $\xi = 0$ to the Landau gauge. The $|q|$ dependence comes from calculating the self energy

$$\text{---} \circlearrowleft \text{---} \quad . \quad (68)$$

The charge e has disappeared from the final result. This charge appears if one includes the q^2 dependence in the denominator of the gauge propagator. But in the small q (long distance) limit, the $|q|$ dependence dominates over q^2 term, no matter how large e is. Another way to say this is that the QED₃ is self-critical. It will flow to a stable fixed point — even if we start with a large gauge charge e — at least for some large N .

The gauge propagator of our theory, *in the leading order*, will come *solely* from the f-fermion bubble, given diagrammatically in Eq. (68). The b propagation does not contribute to the gauge field's self energy in the leading order. Therefore, in the leading order, $\langle a_\mu a_\nu \rangle (q)$ of our Lagrangian density Eq. (61) is the same as QED₃.

The Kondo Field b . The b field propagator, in the leading order, is given by:

$$\langle bb^* \rangle^{-1} (q) \equiv G_b^{-1}(q) = G_{b0}^{-1}(q) - \text{---} \circlearrowleft \text{---} \quad , \quad (69)$$

in two different limits:

$$G_b(0, m_b \rightarrow 0) \propto m_b^{-\gamma_b}, \quad (81)$$

$$G_b(k \rightarrow 0, 0) \propto |k|^{-2+\eta_b}. \quad (82)$$

It should be noted that since b is not gauge invariant, γ_b and η_b are not gauge invariant. However ν by definition, given by Eq. (77), is a gauge invariant quantity. Since it is not a priori obvious that the scaling relation given by Eq. (79) is gauge invariant, we calculate γ_b and η_b in a general gauge, and show that ν derived from Eq. (79) is indeed gauge invariant.

The methods we use to calculate γ_b and η_b are very different. The calculation of γ_b is done by directly calculating the Green's function $G_b(0, m_b)$. Calculating η_b , in this manner, is much more involved. Instead, we calculate η_b by relating η_b to the scaling dimension of $\bar{\Psi}^a \Phi^a$. The scaling dimension of $\bar{\Psi}^a \Phi^a$ is then obtained by perturbing the Lagrangian density $\mathcal{L}_E \rightarrow \mathcal{L}_E + \delta \bar{\Psi}^a \Phi^a$ and applying the Callan-Symanzik equation for the propagator $\langle \bar{\Psi}^a \Phi^a \rangle$, in the presence of the perturbation, to obtain the flow of the composite operator $\bar{\Psi}^a \Phi^a$, and thus extracting its scaling dimension.

1. γ_b

To calculate γ_b we calculate $G_b(0, m_b)$, i.e. the uniform part of the b propagator slightly away from the critical point. From the calculations in the previous section leading to Eq. (71) we have

$$G_b^{-1}(0, m_b) = N \frac{m_b}{4} - \Sigma_b^{1/N}(0, m_b), \quad (83)$$

where $\Sigma_b^{1/N}(0, m_b)$ is given diagrammatically by

$$\begin{aligned} \Sigma_b^{1/N}(0, m_b) &= \text{Diagram 1} \\ &+ \text{Diagram 2} \\ &+ \text{Diagram 3} \\ &+ \text{Diagram 4} \\ &= \frac{\xi - 1}{\pi^2} m_b \log(m_b/\mu). \end{aligned} \quad (84)$$

This results in

$$\begin{aligned} G_b^{-1}(0, m_b) &= N \frac{m_b}{4} \left(1 - \frac{4(\xi - 1)}{N\pi^2} \log(m_b/\mu) \right) \\ &\propto m_b^{1 - \frac{4(\xi - 1)}{\pi^2 N}}, \end{aligned} \quad (85)$$

from which we obtain

$$\gamma_b = 1 - \frac{4(\xi - 1)}{\pi^2 N}. \quad (86)$$

The integrals are evaluated in the dimensional regularization scheme.^{23,25} The mass scale μ in this scheme is introduced to keep track of dimensions in d dimensional integration and plays the role of a UV cutoff. A *simple pole* in the dimension d reflects the *logarithmic divergence* of the original 3 dimensional integration. We only keep track of the IR divergent parts.

We briefly discuss the diagrams involved in $\Sigma_b^{1/N}(0, m_b)$. The first diagram of Eq. (84) has no m_b dependance. The second and third diagrams are equal and are given by:

$$\text{Diagram 1} = -\frac{1}{2\pi^2} m_b \log(m_b/\mu). \quad (87)$$

The last diagram of Eq. (84) contains the vertex that couples b bosons with the gauge field:

$$\begin{aligned} \text{Diagram 4} &= +N \int \frac{d^3 p}{(2\pi)^3} \text{Tr} \left((\not{p} + \not{k})^{-1} \not{p}^{-1} \gamma^\mu (\not{p} - \not{q})^{-1} \right). \end{aligned} \quad (88)$$

In the calculation of $\Sigma_b^{1/N}(0, m)$ the momentum entering this vertex is zero. The result of this integral for $k = 0$ is

$$\int \frac{d^3 p}{(2\pi)^3} \text{Tr} \left(\not{p}^{-1} \not{p}^{-1} \gamma^\mu (\not{p} - \not{q})^{-1} \right) = \frac{-q_\mu}{4|q|}. \quad (89)$$

Having the result of the above integral, we get

$$\sum_{\nu\sigma} \text{Diagram 4} = \frac{\xi}{\pi^2} m_b \log(m_b/\mu). \quad (90)$$

2. η_b

η_b is easily related to the scaling dimension of the b field at the critical point [See Eq. (82)] :

$$\eta_b = -1 + 2[b]. \quad (91)$$

Since the only way for the b field to propagate is to decay into $\bar{\Psi}^a \Phi^a$, the scaling of the *self energy* of b is the same as the *propagator* of the composite operator $\bar{\Psi}^a \Phi^a$. This observation results in

$$[b] = 3 - [\bar{\Psi}^a \Phi^a]. \quad (92)$$

Thus η_b is known once we know the scaling dimension of the composite operator $\bar{\Psi}^a \Phi^a$.

The scaling dimension of $\bar{\Psi}^a \Phi^a$ is obtained by adding the perturbation

$$\mathcal{L}_E \rightarrow \mathcal{L}_E + \delta \bar{\Psi}^a \Phi^a \quad (93)$$

to the Lagrangian density and obtaining the flow of δ by studying the Callan-Symanzik equation for the propagator $\langle \Psi^a(x) \bar{\Phi}^a(x') \rangle$.

The Callan-Symanzik equation is essentially the “scale invariance” relation.^{23,24} Near the fixed point, a change in scale has to be accompanied by the flow of some coupling constants and scaling of the fields to maintain scale invariance. For the propagator under consideration it will read

$$\left(-\frac{\partial}{\partial \ell} - \Delta_\Psi - \Delta_\Phi + \frac{dC_m}{d\ell} \frac{\partial}{\partial C_m} \right) \langle \Psi^a(e^\ell x) \bar{\Phi}^a(e^\ell x') \rangle = 0, \quad (94)$$

where Δ_Φ and Δ_Ψ are scaling dimensions of the fields Φ and Ψ . The set C includes the coupling constants that flow. For the perturbation given by Eq. (93) it has only 1 element:²⁷

$$C = \{\delta\}. \quad (95)$$

It is more convenient to apply the Callan-Symanzik equation to the momentum-space Green’s function $\langle \bar{\Psi}^a \Phi^a \rangle(k)$

$$\langle \Psi^a \bar{\Phi}^a \rangle(k) = \int \frac{d^3 k}{(2\pi)^3} e^{ik(x-x')} \langle \Psi^a(x) \bar{\Phi}^a(x') \rangle. \quad (96)$$

Eq. (94) results in

$$\left(-\frac{\partial}{\partial \ell} + (3 - \Delta_\Psi - \Delta_\Phi) + \frac{d\delta}{d\ell} \frac{\partial}{\partial \delta} \right) \langle \bar{\Psi}^a \Phi^a \rangle(e^{-\ell} k) = 0, \quad (97)$$

where “3” is coming from the scaling of the measure $d^3 k$ in the integrand of Eq. (96).

To apply the Callan-Symanzik equation we first need to obtain Δ_Φ and Δ_Ψ . The gauge dependant Δ_Φ is ob-

tained by calculating the propagator

$$\langle \Phi^a \bar{\Phi}^a \rangle = \text{---} \leftarrow \text{---} + \text{---} \leftarrow \text{---} \leftarrow \text{---} + \text{---} \leftarrow \text{---} \leftarrow \text{---} \leftarrow \text{---} \quad (98)$$

The result is

$$\langle \Phi^a \bar{\Phi}^a \rangle(k) = (ik)^{-1} \left(1 + \frac{1}{N} \left(\frac{2}{\pi^2} + \frac{4}{\pi^2} (\xi - 1) \right) \log(|k|/\mu) \right), \quad (99)$$

from which we get

$$\Delta_\Phi = 1 + \frac{1}{N} \left(\frac{1}{\pi^2} + \frac{2}{\pi^2} (\xi - 1) \right). \quad (100)$$

Similarly, calculating the *gauge invariant* conduction electron propagator

$$\langle \Psi^a \bar{\Psi}^a \rangle = \text{---} \leftarrow \text{---} + \text{---} \leftarrow \text{---} \leftarrow \text{---} \leftarrow \text{---} \quad (101)$$

$$= (ik)^{-1} \left(1 + \frac{2}{3\pi^2 N} \log(|k|/\mu) \right)$$

results in the gauge invariant Δ_Ψ

$$\Delta_\Psi = 1 + \frac{1}{3\pi^2 N}. \quad (102)$$

The logarithmic infrared divergence of Eq. (101) can be interpreted as the scaling of the quasi-particle weight Z , defined by $\langle \Psi^a \bar{\Psi}^a \rangle(k) = Z(ik)^{-1}$. The scaling form of Z which is consistent with Eq. (101) is

$$Z = \left| \frac{k}{\mu} \right|^{\frac{2}{3\pi^2 N}}. \quad (103)$$

The vanishing of the Z factor as $k \rightarrow 0$ can in principle be seen in tunnelling experiments. This non-Fermi liquid behavior arises, because at the KI-ASL fixed point, there are very strong scattering of conduction electrons into the

f-fermions. This is due to the fact that the b field which causes the scattering has become massless.

The next step is to obtain $\langle \bar{\Psi}^a \Phi^a \rangle(k)$ in the presence of the perturbation $\delta \bar{\Psi}^a \Phi^a$ given by Eq. (93). This perturbation is represented diagrammatically by

$$\text{Diagram: Two external lines with arrows pointing left, one with a star, meeting at a vertex.} = \delta. \quad (104)$$

The diagrammatic expression for $\langle \Psi^a \bar{\Phi}^a \rangle$ is then given by

$$\begin{aligned} \langle \Psi^a \bar{\Phi}^a \rangle = & \text{Diagram: Two external lines with arrows pointing left, one with a star, meeting at a vertex.} \\ & + \text{Diagram: Two external lines with arrows pointing left, one with a star, meeting at a vertex, with a loop attached to the right line.} \\ & + \text{Diagram: Two external lines with arrows pointing left, one with a star, meeting at a vertex, with a loop attached to the right line and a dashed line attached to the loop.} \\ & + \text{Diagram: Two external lines with arrows pointing left, one with a star, meeting at a vertex, with a loop attached to the right line and a dashed line attached to the loop.} \\ & + \text{Diagram: Two external lines with arrows pointing left, one with a star, meeting at a vertex, with a loop attached to the right line and a dashed line attached to the loop.} \\ & + \text{Diagram: Two external lines with arrows pointing left, one with a star, meeting at a vertex, with a loop attached to the right line and a dashed line attached to the loop.} \end{aligned} \quad (105)$$

It results in

$$\langle \Psi^a \bar{\Phi}^a \rangle(k) = \delta (ik)^{-2} \left(1 - \frac{4}{3\pi^2 N} \log(|k|/\mu) \right). \quad (106)$$

Callan-Symanzik equation [Eq. (97)] applied to the above propagator results in

$$\frac{d\delta}{d\ell} = \left(1 + \frac{8}{3\pi^2 N} + \frac{2}{\pi^2 N} (\xi - 1) \right) \delta. \quad (107)$$

The above relation together with Eq. (92) yields:

$$[b] = 1 + \frac{1}{N} \left(\frac{8}{3\pi^2} + \frac{2}{\pi^2} (\xi - 1) \right). \quad (108)$$

Combine this with Eq. (91) to get

$$\eta_b = 1 + \frac{1}{N} \left(\frac{16}{3\pi^2} + \frac{4}{\pi^2} (\xi - 1) \right). \quad (109)$$

Collecting what we have obtained for γ_b and η_b given by Eqs. (86) and (109), together with the scaling relation given by Eq. (79), we arrive at the gauge invariant

$$\nu = 1 + \frac{16}{3\pi^2 N}. \quad (110)$$

Note that the $1/N$ fluctuations have brought us *further away* from the generic $1/2 + \mathcal{O}(\epsilon)$ result one would obtain for a stable fixed point in an ϵ expansion (which is an expansion around the gaussian action), assuming there exists such a stable fixed point.

B. Staggered Spin Correlation

We continue the study of the physical properties of our KI-ASL fixed point by obtaining staggered spin $\mathbf{M} = \mathbf{S}_A - \mathbf{S}_B$ correlation *at* the fixed point. The correlation is algebraic and our fixed point is an algebraic spin liquid fixed point.

Since the decay exponent of $\langle \mathbf{M}(x) \cdot \mathbf{M}(x') \rangle$ and $\langle M^+(x) M^-(x') \rangle$ is the same, it suffices to find the scaling dimension of M^+ . In terms of the field operators $M^+(x)$ is

$$M^+(x) = \bar{\Phi}^1(x) \mathcal{M} \Phi^2(x), \quad (111)$$

where \mathcal{M} is 4×4 matrix, which should be obtained from the relation between the field Φ and the microscopic operators developed in Sec. III. Physically 1 and 2 represents \uparrow and \downarrow . In $1/N$ expansion they are 2 indices among many. \mathcal{M} is obtained to be²⁸

$$\mathcal{M} = \mathbf{1} \otimes \sigma_3. \quad (112)$$

We should add this perturbation to the Lagrangian and study its flow. However $\bar{\Phi}^1(x) \mathcal{M} \Phi^2(x)$ mixes with $\bar{\Psi}^1(x) \mathcal{M} \Psi^2(x)$. In other words M^+ is not a scaling operator. Having this in mind, we perturb the Lagrangian density by

$$\delta \mathcal{L}_E = U_+ \bar{\Phi}^1(x) \mathcal{M} \Phi^2(x) + u_+ \bar{\Psi}^1(x) \mathcal{M} \Psi^2(x) \quad (113)$$

and study the Callan-Symanzik equation for the propagators $\langle \Psi^1 \bar{\Psi}^2 \rangle(k)$ and $\langle \Phi^1 \bar{\Phi}^2 \rangle(k)$. The result (obtained in Appendix B) is

$$\frac{\partial}{\partial \ell} \begin{bmatrix} U_+ \\ u_+ \end{bmatrix} = \begin{bmatrix} 1 + \frac{10}{\pi^2 N} & \frac{-2}{\pi^2 N} \\ \frac{-2}{\pi^2 N} & 1 - \frac{2}{3\pi^2 N} \end{bmatrix} \begin{bmatrix} U_+ \\ u_+ \end{bmatrix}. \quad (114)$$

We emphasize that off-diagonal terms make $1/N$ correction to the scaling dimension of the staggered spin. This is because the scaling dimensions of Ψ and Φ are equal

in the infinite N limit. This is similar to the importance of off-diagonal terms in the 1st order *degenerate* perturbation theory in quantum mechanics.

The largest eigenvalue $1 + 2(7 + \sqrt{73})/(3\pi^2 N)$ of above matrix dominates the scaling of M^+ . The *dominant* scaling dimension of M^+ , denoted by $[M^+]$, is then given by

$$[M^+] = 2 - \frac{2(7 + \sqrt{73})}{3\pi^2 N} \approx 2 - \frac{31.1}{3\pi^2 N}. \quad (115)$$

The decay exponent of the correlation function results immediately:

$$\langle M(x) \cdot M(x') \rangle \propto \frac{1}{|x - x'|^{2[M^+]}} + \dots, \quad (116)$$

where the ellipsis denotes the decay with the larger exponent coming from the other eigenvalue of the matrix in Eq. (114).

Finally, we mention a comparison between our result and the Rantner–Wen studies.¹² They studied spin correlations in their large- N QED₃ effective field theory in the Landau gauge. They were interested in the similar bilinear form as we have here with $\mathcal{M} = \mathbf{1}$. In our calculation any bilinear form with the property $[\mathcal{M}, \gamma_\mu] = 0$ has the same scaling dimension. To check our result we turned off all contributions to the exponent coming from terms involving Ψ . The result $[M^+]_{\text{ASL}} = 2 - 32/(3\pi^2 N)$ obtained in Feynman gauge agrees with theirs obtained in Landau gauge. $2[M^+]_{\text{ASL}}$ corresponds to the decay exponent of localized spin correlation when we are in the ASL phase, where the Kondo field is massive. As expected, we have $[M^+]_{\text{ASL}} < [M^+]$, i.e. the Neel fluctuations are stronger in the ASL phase than at the KI transition, where the Kondo singlets are forming.

In the $J < J_K^{\text{cr}}$ regime the ASL is in the presence of the semi-metal (described by Ψ field) and the gapped Kondo field b . The question may arise whether the semimetal would destabilize the ASL. The semimetal will not destabilize the ASL, because integrating out Ψ and b fields in this phase will produce (retarded) four-fermion interaction term among Φ fields. These four-fermion interactions are irrelevant at the ASL fixed point.

VI. STABILITY OF THE FIXED POINT

In this section we discuss the issue of the stability of the KI–ASL fixed point in the honeycomb lattice to 1st order in $1/N$. There are two separate issues one has to consider in the stability of this fixed point.

In going to the continuum limit we have dropped the compact character of the gauge field. This is only justified if the instanton events, where the flux of the gauge field suddenly changes by 2π , do not proliferate. For $J_K > J_K^{\text{cr}}$ the Kondo field b is condensed and we are in the Higgs phase. Gauge field is massive, its fluctuations are suppressed and instantons do not proliferate.

Addressing the proliferation of instantons in the regime where the Kondo phase has disappeared is more subtle. We know from Polyakov's work that the compact *pure* gauge theory in 2+1 dimension is in the confining phase for all coupling constant, i.e. for all coupling constants the instantons proliferate.²¹ It has been argued recently that coupling the gauge field to massless Dirac fields results in a deconfined phase for sufficiently large N .¹³ This is due to the fact that the massless matter field, in this case Dirac fields, suppress the fluctuations of the gauge field. We apply that argument here and assume that the gauge field in the $J_K < J_K^{\text{cr}}$ regime is in a deconfined phase. At the KI–ASL fixed point, due to the presence of an extra massless matter field, i.e. the Kondo field b , the gauge field fluctuations are suppressed even more.

Next we focus on the instanton–free sector. At the fixed point the gauge field a_μ , boson b and two fermion fields Ψ, Φ ; all have scaling dimension $1 + \mathcal{O}(1/N)$. This can be seen by the form of propagators derived in Sec. IV. The large N scaling dimension of a_μ , b , Ψ and Φ will limit our choices for relevant perturbations. Different such perturbations are discussed below:

- b mass term: this term is already present in the microscopic bare Lagrangian. We have to *tune* J_K to make the effective mass of the b field to be zero. This perturbation is indeed relevant.
- Ψ and Φ mass terms: these mass terms either break the SU(N) flavor symmetry or the particle-hole and rotation symmetry.
- b kinetic term of the form $b^* (\partial_\mu + ia_\mu) b$: this term violates the particle–hole symmetry. It has to be accompanied by $b(\partial_\mu - ia_\mu)b^*$ with an equal coefficient. But $b^* \partial_\mu b + b \partial_\mu b^* = \partial_\mu (b^* b)$ is a total derivative.
- b kinetic term of the form $\delta\mathcal{L} = Ng|(\partial_\mu + ia_\mu)b|^2$: this term is irrelevant by the power counting. That is

$$\frac{dg}{dl} = (-1 + \mathcal{O}(1/N))g.$$

- Kinetic terms for Ψ and Φ fields: these are the only potentially dangerous perturbations, because they are marginal in the $N \rightarrow \infty$ limit. Actually in the derivation of the Lagrangian density Eq. (61) we set $v_c = v_f$ to make the action Lorentz invariant. We have to consider perturbations that break this “tuned” Lorentz symmetry and study their flow. By scaling argument the flow of these perturbations is marginal to first order in $1/N$: marginally irrelevant, relevant, or exactly marginal. Our calculations results in the marginal irrelevance of these types of perturbations. We discuss this issue below.

We break the Lorentz symmetry by adding the perturbation

$$\delta\mathcal{L}_E^a = \sum_\sigma \left(\delta_\sigma \bar{\Psi}^a \gamma_\sigma \partial_\sigma \Psi^a + \Delta_\sigma \bar{\Phi}^a \gamma_\sigma (\partial_\sigma - ia_\sigma) \Phi^a \right)$$

to the Lagrangian density. The perturbation has to be considered both in Ψ and Φ fields because of their mixing due to the exchange of the b field. Applying Callan-Symanzik equation to the propagators $\langle \Psi^a \bar{\Psi}^a \rangle$ and $\langle \Phi^a \bar{\Phi}^a \rangle$ results in the following RG flow:

$$\frac{\partial}{\partial \ell} \begin{bmatrix} \Delta_0 \\ \Delta_1 \\ \Delta_2 \\ \delta_0 \\ \delta_1 \\ \delta_2 \end{bmatrix} = \mathcal{D} \begin{bmatrix} \Delta_0 \\ \Delta_1 \\ \Delta_2 \\ \delta_0 \\ \delta_1 \\ \delta_2 \end{bmatrix}, \quad (117)$$

where the matrix anomalous dimension \mathcal{D} is given by

$$\mathcal{D} = \frac{1}{15\pi^2 N} \begin{bmatrix} -74 & 32 & 32 & -2 & -4 & -4 \\ 32 & -74 & 32 & -4 & -2 & -4 \\ 32 & 32 & -74 & -4 & -4 & -2 \\ -2 & -4 & -4 & -10 & 0 & 0 \\ -4 & -2 & -4 & 0 & -10 & 0 \\ -4 & -4 & -2 & 0 & 0 & -10 \end{bmatrix}. \quad (118)$$

Eigenvalues of this matrix anomalous dimension are all negative except for one trivial zero eigenvalue. The zero eigenvalue is trivial since the corresponding perturbation can be absorbed by scaling Ψ and Φ fields, shown in Appendix A.

We knew from the mean-field result that there exist a fixed point in the parameter space. But our results goes further by ruling out a multi-critical fixed point. So based on our result, for large enough N , this quantum critical point will be achieved by tuning one parameter J_K .

VII. CONCLUSIONS

We have studied the Kondo–Heisenberg model on the honeycomb lattice at half filling. The main motivation for our study is that the Kondo band gap vanishes at a finite Kondo coupling constant (even as $J_H \rightarrow 0$) so that a novel kind of quantum phase transition becomes possible.

In this paper we considered the transition of this Kondo insulator (KI) to a spin liquid phase which is later identified to be algebraic spin liquid (ASL). We developed a mean-field theory for such a transition using a fermionic representation for spins. To consider fluctuations about this mean-field systematically, we adopted a large N generalization of our model by having N spin-flavors rather than just $\{\uparrow, \downarrow\}$. We found that the KI–ASL transition is controlled by a stable Lorentz invariant fixed point. In the Kondo insulator phase, the Kondo field b condenses and we are in the Higgs phase where the gauge field is massive. ASL phase is described by “decoupled” QED₃ (coming from $J_H \mathbf{S}_i \cdot \mathbf{S}_j$ interaction) and the Dirac conduction electrons (coming from the kinetic term for conduction electrons). They are “decoupled” in that the Kondo field that couples these two terms is now massive. For the gauge field, this is a Higgs–deconfinement transition.

We were able to calculate the exponent $\nu = 1 + 16/(3\pi^2 N)$ of the diverging length scale near the transition. Interestingly, $1/N$ fluctuations have pushed the infinite N result further away from the result $\nu = 1/2$ one would get from the Landau-type expansion. We noted that at our fixed point the quasi-particle weight of the conduction electron vanishes which is indicative of non-Fermi liquid behavior. We also calculated the decay exponent of the staggered spin $\mathbf{M} = \mathbf{S}_A - \mathbf{S}_B$ correlation at the fixed point. This is not a scaling operator, since it mixes with $\mathbf{m} = \mathbf{s}_A - \mathbf{s}_B$. The dominant decay exponent turned out to be $2[M^+] = 4 - 4(7 + \sqrt{73})/(3\pi^2 N) \approx 4 - 62.2/(3\pi^2 N)$. On the other hand, in the ASL phase \mathbf{M} is a scaling operator with the decay exponent $2[M^+]_{\text{ASL}} = 4 - 64/(3\pi^2 N)$. The *jump* in this exponent, as one gets to the KI transition point, is due to the fact that there exists an extra massless matter field at the transition (in this case Kondo field b), which modifies the exponent. This jump and its significance was discussed in a different context recently.¹⁸

In connection to this work, we are currently pursuing the numerical study of this model; using a quantum Monte Carlo technique without the fermion sign problem.

VIII. ACKNOWLEDGMENTS

We thank Michael Hermele for many insightful comments and suggestions and we thank T. Senthil and X.-G. Wen for helpful discussions. PAL acknowledges the

support by the Department of Energy under grant DE-FG02-03ER46076.

$\langle \Psi^a \bar{\Psi}^a \rangle$ is given by

$$\langle \Psi^a \bar{\Psi}^a \rangle = \text{---} \rightarrow \text{---}$$

APPENDIX A: RESTORATION OF THE LORENTZ INVARIANCE

Here we will give more details regarding the irrelevance of the perturbations that break the Lorentz symmetry at our Lorentz invariant KI-ASL fixed point. It is tempting to break the Lorentz invariance by perturbing only one field, Ψ or Φ . However Ψ and Φ lose their own identity as b becomes massless and they mix together. Having this mixing in mind we consider the most general perturbation which is of the kinetic form for the Ψ and Φ fields, and is consistent with the gauge symmetry

$$\delta\mathcal{L}_E^a = \sum_{\sigma} \left(\delta_{\sigma} \bar{\Psi}^a \gamma_{\sigma} \partial_{\sigma} \Psi^a + \Delta_{\sigma} \bar{\Phi}^a \gamma_{\sigma} (\partial_{\sigma} - i a_{\sigma}) \Phi^a \right). \quad (\text{A1})$$

The corrections to fermion propagators and gauge vortex is represented diagrammatically:

$$\begin{aligned} \text{---} \xrightarrow{q} \text{---} \xrightarrow{q} \text{---} \xrightarrow{\sigma} \text{---} &= -i\delta_{\sigma} \not{q}_{\sigma}, \\ \text{---} \xrightarrow{q} \text{---} \xrightarrow{\sigma} \text{---} \xrightarrow{q} \text{---} &= -i\Delta_{\sigma} \not{q}_{\sigma}, \\ \text{---} \xrightarrow{\sigma} \text{---} \xrightarrow{\text{---}} \text{---} &= +i\Delta_{\sigma} \gamma_{\sigma}, \end{aligned} \quad (\text{A2})$$

$$\begin{aligned} \langle \Psi^a \bar{\Psi}^a \rangle = & \text{---} \rightarrow \text{---} \\ & + \text{---} \rightarrow \text{---} \xrightarrow{\text{---}} \text{---} \\ & + \text{---} \rightarrow \text{---} \xrightarrow{\sigma} \text{---} \\ & + \text{---} \rightarrow \text{---} \xrightarrow{\sigma} \text{---} \xrightarrow{\sigma} \text{---} \\ & + \text{---} \rightarrow \text{---} \xrightarrow{\sigma} \text{---} \xrightarrow{\sigma} \text{---} \xrightarrow{\sigma} \text{---}, \end{aligned} \quad (\text{A4})$$

where the sum over the space-time index σ , appearing in the above diagrams, is understood. Calculation of the diagrams — done in Feynman gauge — results in:

$$\begin{aligned} \langle \Psi^a \bar{\Psi}^a \rangle (k) = & -i\mathbb{k}^{-1} \left(1 + \frac{2}{3\pi^2 N} \log(|k|/\mu) \right) \\ & + i\mathbb{k}^{-1} \mathbb{k}_{\sigma} \mathbb{k}^{-1} \left(\delta_{\sigma} + \frac{\log(|k|/\mu)}{15\pi^2 N} |\epsilon_{\sigma\mu\nu}| S_{\sigma;\mu\nu} \right), \end{aligned} \quad (\text{A5})$$

where $S_{\sigma;\mu\nu}$ is given by

$$S_{\sigma;\mu\nu} = 20\delta_{\sigma} + 2\Delta_{\sigma} + 4\Delta_{\mu} + 4\Delta_{\nu}. \quad (\text{A6})$$

where we have used the notation

$$\not{q}_{\sigma} \equiv q_{\sigma} \gamma_{\sigma}. \quad (\text{A3})$$

The above propagator has a contribution from the unperturbed fixed-point action, which gives the gauge independent scaling dimension for Ψ field

$$\Delta_{\Psi} = 1 + \frac{1}{3\pi^2 N}. \quad (\text{A7})$$

We evaluate the two propagators $\langle \Psi^a \bar{\Psi}^a \rangle$ and $\langle \Phi^a \bar{\Phi}^a \rangle$ in the presence of the perturbation given by Eq. (A1).

Next we calculate $\langle \Phi^a \bar{\Phi}^a \rangle$ which is given by

We obtain

$$\begin{aligned} \langle \Phi^a \bar{\Phi}^a \rangle(k) &= -i \not{k}^{-1} \left(1 + \frac{2}{\pi^2 N} \log(|k|/\mu) \right) \\ &+ i \not{k}^{-1} \not{k}_\sigma \not{k}^{-1} \left(\Delta_\sigma + \frac{\log(|k|/\mu)}{15\pi^2 N} |\epsilon_{\sigma\mu\nu}| F_{\sigma;\mu\nu} \right), \end{aligned} \quad (\text{A9})$$

where $F_{\sigma;\mu\nu}$ is given by

$$F_{\sigma;\mu\nu} = 104\Delta_\sigma - 32\Delta_\mu - 32\Delta_\nu + 2\delta_\sigma + 4\delta_\mu + 4\delta_\nu. \quad (\text{A10})$$

From Eq. (A9), we obtain the scaling dimension of the Φ field in Feynman gauge :

$$\Delta_\Phi = 1 + \frac{1}{\pi^2 N}. \quad (\text{A11})$$

Then we use the Callan-Symanzik equation machinery by scaling the momentum $k \rightarrow e^{-\ell}k$ and applying

$$\left(-\frac{\partial}{\partial \ell} + (3 - 2\Delta_{\Psi}) + \frac{dC_m}{d\ell} \frac{\partial}{\partial C_m} \right) \langle \Psi^a \bar{\Psi}^a \rangle = 0, \quad (\text{A12})$$

$$\left(-\frac{\partial}{\partial \ell} + (3 - 2\Delta_\Phi) + \frac{dC_m}{d\ell} \frac{\partial}{\partial C_m} \right) \langle \Phi^a \bar{\Phi}^a \rangle = 0, \quad (\text{A13})$$

where the set C includes the coupling constants that flow. For the perturbation under consideration it has 6 elements:

$$C = \{\Delta_0, \Delta_1, \Delta_2, \delta_0, \delta_1, \delta_2\}.$$

Eqs. (A12), and (A13) will lead to the RG flow :

$$\frac{\partial}{\partial \ell} \begin{bmatrix} \Delta_0 \\ \Delta_1 \\ \Delta_2 \\ \delta_0 \\ \delta_1 \\ \delta_2 \end{bmatrix} = \mathcal{D} \begin{bmatrix} \Delta_0 \\ \Delta_1 \\ \Delta_2 \\ \delta_0 \\ \delta_1 \\ \delta_2 \end{bmatrix}, \quad (\text{A14})$$

where the matrix anomalous dimension \mathcal{D} is given by

$$\mathcal{D} = \frac{1}{15\pi^2 N} \begin{bmatrix} -74 & 32 & 32 & -2 & -4 & -4 \\ 32 & -74 & 32 & -4 & -2 & -4 \\ 32 & 32 & -74 & -4 & -4 & -2 \\ -2 & -4 & -4 & -10 & 0 & 0 \\ -4 & -2 & -4 & 0 & -10 & 0 \\ -4 & -4 & -2 & 0 & 0 & -10 \end{bmatrix}. \quad (\text{A15})$$

All the eigenvalues of this matrix anomalous dimension is nonpositive. There is one zero eigenvalue with the corresponding eigenvector

$$\begin{bmatrix} \Delta \\ \Delta \\ \Delta \\ -\Delta \\ -\Delta \\ -\Delta \end{bmatrix}.$$

The above shift can be absorbed by scaling Ψ and Φ fields separately. The scaling is *delicate*, since in our RG scheme we have fixed the coefficient of $(b\bar{\Psi}^a\Phi^a + c.c.)$ to be 1. So the scaling of Ψ and Φ has to be accompanied by an appropriate scaling of b . But this - in general - will move us away from the critical point. For the above perturbation though, the scaling factor for b is 1:

$$\frac{1}{\sqrt{1-\Delta}\sqrt{1+\Delta}} = 1 + \mathcal{O}(\Delta^2).$$

So the above perturbation remains *exactly marginal* to all orders in $1/N$.

It is interesting to note that the uniform shift

$$\begin{bmatrix} \Delta \\ \Delta \\ \Delta \\ \Delta \\ \Delta \\ \Delta \end{bmatrix}$$

is an eigenvector with a negative eigenvalue. Why should this perturbation flow? The absorption of the uniform perturbation in Ψ and Φ has to be accompanied by scaling the b field by

$$\frac{1}{\sqrt{1+\Delta}\sqrt{1+\Delta}} = 1 - \Delta + \mathcal{O}(\Delta^2). \quad (\text{A16})$$

This scaling of the b field will move us away from the critical point.

APPENDIX B: STAGGERED SPIN CORRELATION

In this appendix we will find the algebraic decay exponent of $\langle \mathbf{M}(x) \cdot \mathbf{M}(x') \rangle$ at KI-ASL fixed point. We do this by obtaining the staggered spin \mathbf{M} scaling dimension. It suffices to find the scaling dimension of M^+ , since the decay exponent of $\langle \mathbf{M}(x) \cdot \mathbf{M}(x') \rangle$ and $\langle M^+(x)M^-(x') \rangle$ is the same. The first step is to translate M^+ to the field theory language with the dictionary provided by Eq. 53. The expanded form is given by

$$\Phi = \begin{bmatrix} f_{A+} \\ -f_{B+} \\ -if_{B-} \\ -if_{A-} \end{bmatrix} \quad (B1)$$

$$\bar{\Phi} = \begin{bmatrix} f_{A+}^\dagger & f_{B+}^\dagger & i f_{B-}^\dagger & -i f_{A-}^\dagger \end{bmatrix} \quad (B2)$$

Start with the expression for $S_A^+ = S_A^1 + iS_A^2 = f_A^{1\dagger} f_A^2$, which leads to

$$S_A^+(x) = \bar{\Phi}^1(x) \begin{pmatrix} 1 & & & \\ & 0 & & \\ & & 0 & \\ & & & -1 \end{pmatrix} \Phi^2(x). \quad (B3)$$

The similar translation can be done for S_B^+ . The final result is:

$$M^+(x) = \Phi^1(x)\mathcal{M}\Phi^2(x), \quad (B4)$$

where \mathcal{M} is

$$\mathcal{M} = \begin{pmatrix} 1 & & & \\ & 1 & & \\ & & -1 & \\ & & & -1 \end{pmatrix} = \mathbf{1} \otimes \sigma_3. \quad (B5)$$

The matrix \mathcal{M} has the following properties:

$$[\mathcal{M}, \gamma_\mu] = 0, \quad (B6)$$

$$\mathrm{Tr}(\mathcal{M}\Gamma) = 0, \quad (B7)$$

where Γ is a generic notation representing *any* number of γ_μ matrices multiplied. The 1st property is useful since \mathcal{M} passes through all the γ matrices and the final result for the propagators $\langle \Phi_i^1 \bar{\Phi}_j^2 \rangle$ and $\langle \Psi_i^1 \bar{\Psi}_j^2 \rangle$ will have a simple matrix form $(\not{k}^{-1} \mathcal{M} \not{k}^{-1})_{ij}$. The second property causes any diagram, with matrix \mathcal{M} left in a loop, to vanish.

The scaling dimension of M^+ is obtained by looking at its relevant flow near the fixed point. Due to mixing we perturb the Lagrangian density by

$$\delta\mathcal{L}_E = U_+ \bar{\Phi}^1(x) \mathcal{M} \Phi^2(x) + u_+ \bar{\Psi}^1(x) \mathcal{M} \Psi^2(x), \quad (\text{B8})$$

and study the Callan-Symanzik equation for the propagators $\langle \Phi^1 \bar{\Phi}^2 \rangle$ and $\langle \Psi^1 \bar{\Psi}^2 \rangle$.

The vertices corresponding to these perturbations are represented by

$$\begin{array}{c} \text{Diagram:} \\ \text{A horizontal line with two arrows pointing right. Between the arrows is a diamond-shaped vertex. Above the first arrow is the label '1' and above the second arrow is the label '2'.} \end{array} = U_+ \mathcal{M} \quad (\text{B9})$$

The diagrammatic expression for propagators $\langle \Phi^1 \bar{\Phi}^2 \rangle$

and $\langle \Psi^1 \bar{\Psi}^2 \rangle$ is then given by:

$$\begin{aligned}
 \langle \Psi^1 \bar{\Psi}^2 \rangle = & \quad \text{Diagram 1: Two horizontal lines with arrows pointing right, a diamond vertex, and a black dot.} \\
 + & \quad \text{Diagram 2: Two horizontal lines with arrows pointing right, a diamond vertex, and a dashed loop.} \\
 + & \quad \text{Diagram 3: Two horizontal lines with arrows pointing right, a dashed loop, and a diamond vertex.} \\
 + & \quad \text{Diagram 4: Two horizontal lines with arrows pointing right, a black dot, and a dashed loop.}
 \end{aligned}$$

(B10)

The final answers in the Feynman gauge are as follows:

$$\begin{aligned} \langle \Psi^1 \bar{\Psi}^2 \rangle(k) = -\not{k}^{-1} \mathcal{M} \not{k}^{-1} & \left(u_+ \left(1 + \frac{4}{3\pi^2 N} \log(|k|/\mu) \right) \right. \\ & \left. + \frac{2U_+}{\pi^2 N} \log(|k|/\mu) \right), \quad (\text{B12}) \end{aligned}$$

$$\begin{aligned} \langle \Phi^1 \bar{\Phi}^2 \rangle(k) = -\not{k}^{-1} \mathcal{M} \not{k}^{-1} & \left(U_+ \left(1 - \frac{8}{\pi^2 N} \log(|k|/\mu) \right) \right. \\ & \left. + \frac{2u_+}{\pi^2 N} \log(|k|/\mu) \right). \quad (\text{B13}) \end{aligned}$$

Then we use the Callan-Symanzik equation by scaling the momentum $k \rightarrow e^{-\ell}k$ and applying

$$\begin{aligned} \left(-\frac{\partial}{\partial \ell} + (3 - 2\Delta_\Psi) + \frac{dC_m}{d\ell} \frac{\partial}{\partial C_m} \right) \langle \Psi^1 \bar{\Psi}^2 \rangle &= 0 \\ \left(-\frac{\partial}{\partial \ell} + (3 - 2\Delta_\Phi) + \frac{dC_m}{d\ell} \frac{\partial}{\partial C_m} \right) \langle \Phi^1 \bar{\Phi}^2 \rangle &= 0 \end{aligned} \quad (B14)$$

The set C includes the coupling constants that flow. For the perturbation under consideration it has two elements:

$$C = \{U_+, u_+\}.$$

The above Callan-Symanzik equations leads to the RG flow :

$$\frac{\partial}{\partial \ell} \begin{bmatrix} U_+ \\ u_+ \end{bmatrix} = \begin{bmatrix} 1 + \frac{10}{\pi^2 N} & \frac{-2}{\pi^2 N} \\ \frac{-2}{\pi^2 N} & 1 - \frac{2}{3\pi^2 N} \end{bmatrix} \begin{bmatrix} U_+ \\ u_+ \end{bmatrix}. \quad (\text{B15})$$

$$\begin{aligned}
 \langle \Phi^1 \bar{\Phi}^2 \rangle = & \text{ (Diagram 1: A horizontal line with a diamond at the right end and an arrow pointing left, followed by a double-headed arrow.)} \\
 + & \text{ (Diagram 2: A horizontal line with a diamond at the second vertex from the left, followed by a wavy line, a dot, and an arrow pointing right, then a double-headed arrow.)} \\
 + & \text{ (Diagram 3: A horizontal line with a wavy line, a dot, and an arrow pointing right, followed by a double-headed arrow, then a diamond at the right end and an arrow pointing left.)} \\
 + & \text{ (Diagram 4: A horizontal line with a wavy line, a dot, and an arrow pointing right, followed by a double-headed arrow, then a diamond at the second vertex from the right and an arrow pointing left.)}
 \end{aligned}$$

(B11)

¹ P. Coleman, and A. J. Schofield, *Nature* **433**, 226-229 (2005).

² J. Hertz, *Phys. Rev. B* **14**, 1165 (1976); T. Moriya, *Spin Fluctuations in Itinerant Electron Magnetism*, Springer-Verlag, Berlin (1985); A. J. Millis, *Phys. Rev. B* **48**, 7183 (1993).

³ T. Senthil, S. Sachdev, and M. Vojta, *Phys. Rev. Lett.* **90**, 216403 (2003); T. Senthil, M. Vojta, and S. Sachdev, *Phys. Rev. B* **69**, 035111 (2004).

⁴ T. Senthil, S. Sachdev, and M. Vojta, *Physica B* 359-361, 9 (2005).

⁵ P. Coleman, J.B. Marston, A.J. Schofield, *Phys. Rev. B* **72** (2005) 245111.

⁶ I. Paul, C. Pepin, and M. R. Norman, cond-mat/0605152.

⁷ C. Cassanello, and E. Fradkin, *Phys. Rev. B* **53**, 15079 (1996).

⁸ K. S. D. Beach, P. A. Lee, and P. Monthoux, *Phys. Rev. Lett.* **92**, 026401 (2004).

⁹ F.F. Assaad, *Phys. Rev. Lett.* **83**, 796 (1999).

¹⁰ T. Senthil, A. Vishwanath, L. Balents, S. Sachdev, and M. P. A. Fisher, *Science* **303**, 1490 (2004); T. Senthil, L. Balents, S. Sachdev, A. Vishwanath, and M. P. A. Fisher, *Phys. Rev. B* **70**, 144407 (2004).

¹¹ I. Affleck, and J. B. Marston, *Phys. Rev. B* **37**, 3774 (1988); J. B. Marston, and I. Affleck, *Phys. Rev. B* **39**, 11538 (1989).

¹² W. Rantner, and X.-G. Wen, *Phys. Rev. B* **66**, 144501 (2002).

¹³ M. Hermele, T. Senthil, M. P. A. Fisher, P. A. Lee, N. Nagaosa, and X.-G. Wen, *Phys. Rev. B* **70**, 214437 (2004).

¹⁴ M. Hermele, T. Senthil, and M. P. A. Fisher, *Phys. Rev. B* **72**, 104404 (2005).

¹⁵ O. Vafek, Z. Tesanovic, and M. Franz, *Phys. Rev. Lett.* **89**, 157003 (2002).

¹⁶ T. W. Appelquist, M. Bowick, D. Karabali, and L. C. R. Wijewardhana, *Phys. Rev. D* **33**, 3704 (1986).

¹⁷ X.-G. Wen, *Phys. Rev. B* **65**, 165113 (2002).

¹⁸ Y. Ran, and X.-G. Wen, *Phys. Rev. Lett.* **96**, 026802 (2006).

¹⁹ J. B. Kogut, *Rev. Mod. Phys.* **51**, 659 (1979).

²⁰ S. K. Ma, *Modern Theory of Critical Phenomena* (Benjamin, New York, 1976).

²¹ A. M. Polyakov, *Gauge Fields and Strings* (Harwood, New York, 1987).

²² J. W. Negele, and H. Orland, *Quantum Many-Particle Systems* (Addison-Wesley, New York, 1988).

²³ L. S. Brown, *Quantum Field Theory* (Cambridge University Press, Cambridge, UK, 1992).

²⁴ S. Coleman, *Aspects of Symmetry* (Cambridge University Press, Cambridge, UK, 1985).

²⁵ J. C. Collins, *Renormalization* (Cambridge University Press, Cambridge, UK, 1986).

²⁶ See Fig. 6 of the mentioned Assaad's paper.

²⁷ $\bar{\Psi}^a \Phi^a$ and $\bar{\Phi}^a \Psi^a$ have different gauge charges and they do not mix together.

²⁸ See the Appendix B.